**Supporting Information**

# MOFs-Derived Zn-Doped Ceria/rGO Nanocomposites as Photoanode for Solar-Driven Water Splitting

Pramod A. Koyale[a], Amruta D. Patil[b], Tukaram D. Dongale[b], Parth S. Thorat[c], Santosh S. Sutar[d], Vinayak G. Parale[e], Hyung-Ho Park[e], Dillip K. Panda[f], and Sagar D. Delekar[a,*]

a. Department of Chemistry, Shivaji University, Kolhapur, Maharashtra, 416004, India
b. School of Nanoscience and Biotechnology, Shivaji University, Kolhapur, Maharashtra, 416004, India
c. Department of Statistics, Shivaji University, Kolhapur, Maharashtra, 416004, India
d. Yashwantrao Chavan School of Rural Development, Shivaji University, Kolhapur, Maharashtra, 416004, India
e. Department of Materials Science and Engineering, Yonsei University, Seoul 03722, Republic of Korea
f. Department of Materials Science and Engineering, Clemson University, Clemson, South Carolina 29631, United States

**Corresponding Author**

E-mail: sdd_chem@unishivaji.ac.in

## Materials

Potassium permanganate ($KMnO_4$), cerium (III) nitrate hexahydrate [$Ce(NO_3)_3.6H_2O$], benzene-1,3,5-tricarboxylic acid (BTC, Trimesic acid), N, N-Dimethylformamide (DMF), ethanol, zinc acetate [$(CH_3COO)_2Zn.2H_2O$], sulfuric acid ($H_2SO_4$), phosphoric acid ($H_3PO_4$), hydrazine hydrate, sodium borohydrid ($NaBH_4$), hydrochloric acid (HCl), hydrogen peroxide ($H_2O_2$), and acetonitrile (ACN) are the chemicals, purchased from sigma Aldrich, India. In addition, the conducting substrate i.e., nickel foam (NF) was also purchased from Sigma Aldrich, India.

## Synthesis of Graphene Oxide (GO)

To synthesize the graphene oxide (GO), earlier reported Hummer's method was employed. Within the solution of conc. $H_2SO_4$ and $H_3PO_4$ (having a molar ratio of 9:1), 2 gm of graphite powder was dissolved with continuous stirring followed by an addition of some quantity of $KMnO_4$. Thereafter, the stirring was continued for the next 8 hrs. until the color of the suspension turned slightly green. Then, an excess amount of $KMnO_4$ with 30% $H_2O_2$ was added gradually to the said reaction mixture under constant stirring. Afterward, the said reaction was acidified using dilute HCl. The final product was obtained followed by a centrifuge of the solution, washing, and desiccating overnight at around 100$^oC$.

## Synthesis of Reduced Graphene Oxide (rGO)

The 'as prepared' GO powder (100 mg) was placed in a round-bottom flask with an equivalent amount of water to produce a yellow-brown dispersion. This solution was further sonicated using a bath sonicator until it became clean. Thereafter, the said solution was heated in an oil bath at 120$^oC$ with the addition of 1 mL of hydrazine hydrate and $NaBH_4$ under continuous stirring for the next 24 hrs. (the entire setup was maintained cold by a water-cooled condenser). The black precipitate was formed, which was rinsed in water as well as ethanol and then dried to form a rGO powder.[1]

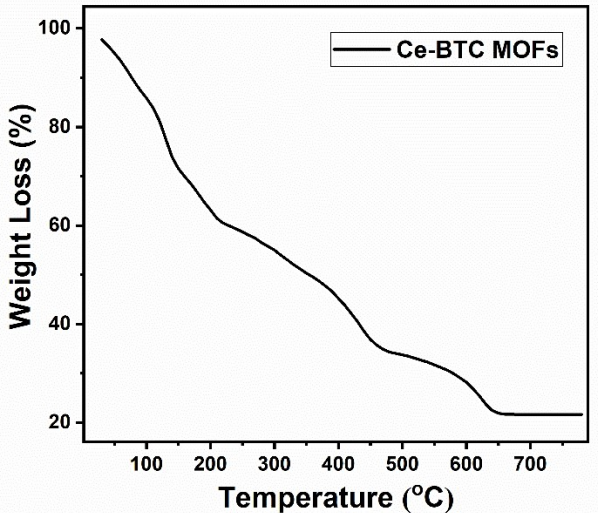


**Figure S1**. TGA curve of Ce-BTC MOFs.

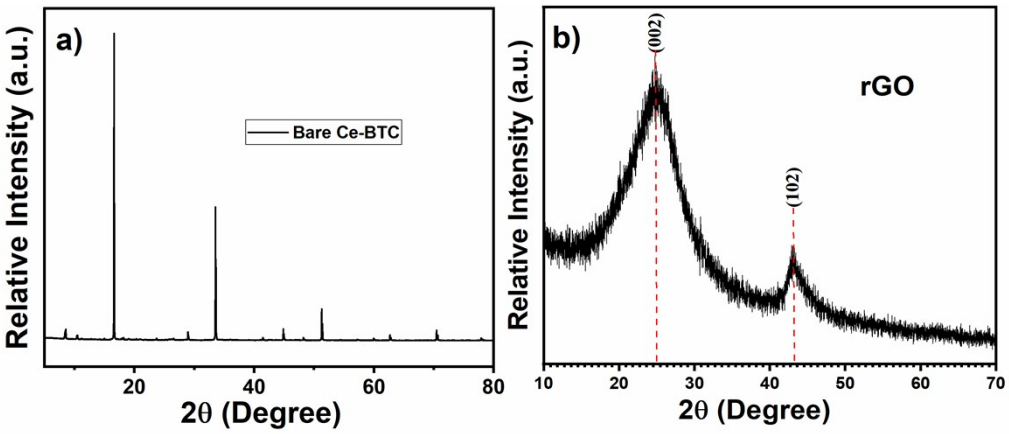


**Figure S2**. XRD patterns: a) bare Ce-BTC MOFs, and b) rGO.

The slight red shift is observed for ZCR-3 NCs as compared to 3-Zn-$CeO_2$ NCs as well as bare $CeO_2$ NBs, showing the better optical property for the same along with a reduced band gap of 2.72 eV from that of 3-Zn-$CeO_2$ NCs (2.75 eV) and bare $CeO_2$ NBs (2.86 eV). Hence, such modification of bare $CeO_2$ NBs is favorable for solar energy studies having improved optical belongings. PL spectra for optimized samples in the wavelength range of 425 nm to 525 nm are shown in **Figure S4**. With the application of an excitation wavelength of 295 nm, broad emission peaks were observed for all samples (within the said range of wavelength), whereas these are projecting similarly in all samples. These emission bands between 425 and 525 nm can signify the existence of oxygen vacancies within the samples.[2] Such vacancies can accomplish more valence electrons which can quickly get excited and trapped in the defect

centres.[3] Herein, the PL intensity of bare $CeO_2$ NBs decreases with increase an in the incorporation of $Zn^{2+}$ ion and rGO, which diminishes the rate of recombination of photogenerated electron-hole pairs. So, there can be several photogenerated electrons and holes for the redox reaction. Therefore, better interfacial charge transfer between the materials is possible with the help of such designed NCs.

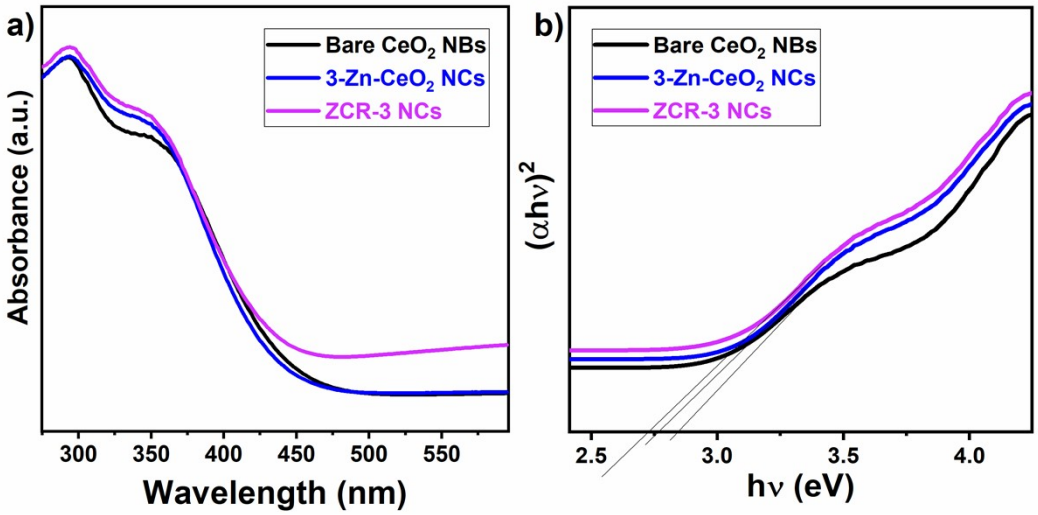


**Figure S3.** a) UV-visible spectra and b) Tauc plot for the band gap calculation for bare $CeO_2$ NBs, 3-Zn-$CeO_2$ NCs, and ZCR-3 NCs.

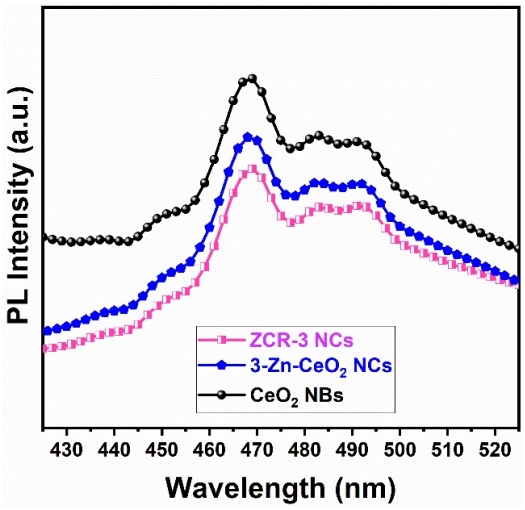


**Figure S4.** Photoluminescence spectra at an excitation wavelength of 295 nm for bare $CeO_2$ NBs, 3-Zn-$CeO_2$ NCs, and ZCR-3 NCs.

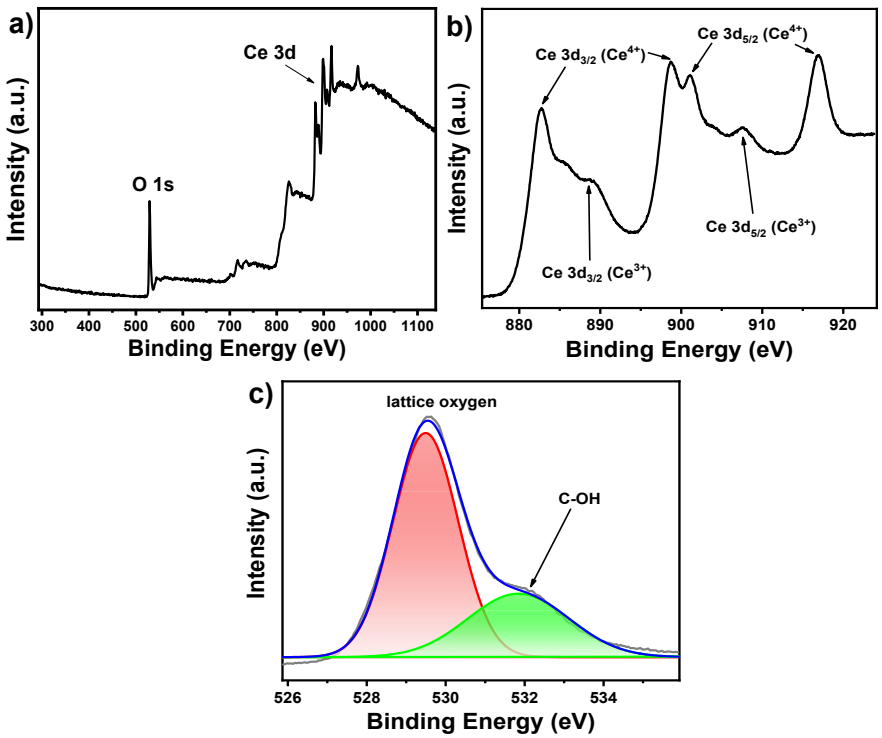


**Figure S5**. a) XPS survey spectrum of $CeO_2$. High-resolution core level XPS spectra for b) Ce 3d, and c) O 1s.

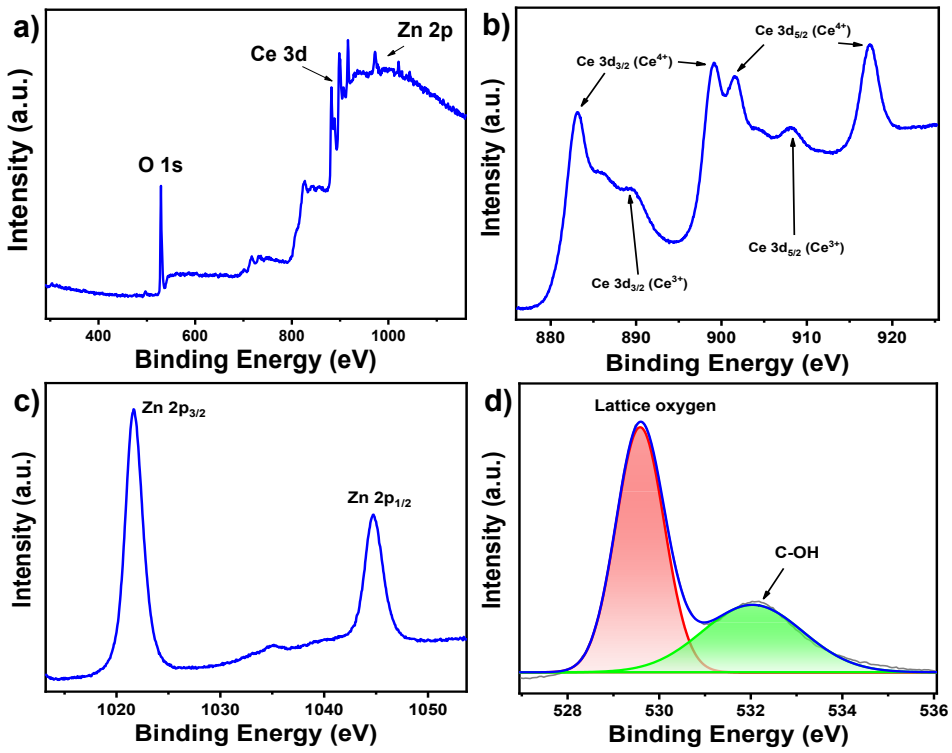


**Figure S6**. a) XPS survey spectrum of Zn-$CeO_2$. High-resolution core level XPS spectra for b) Ce 3d, c) Zn 2p, and d) O 1s.

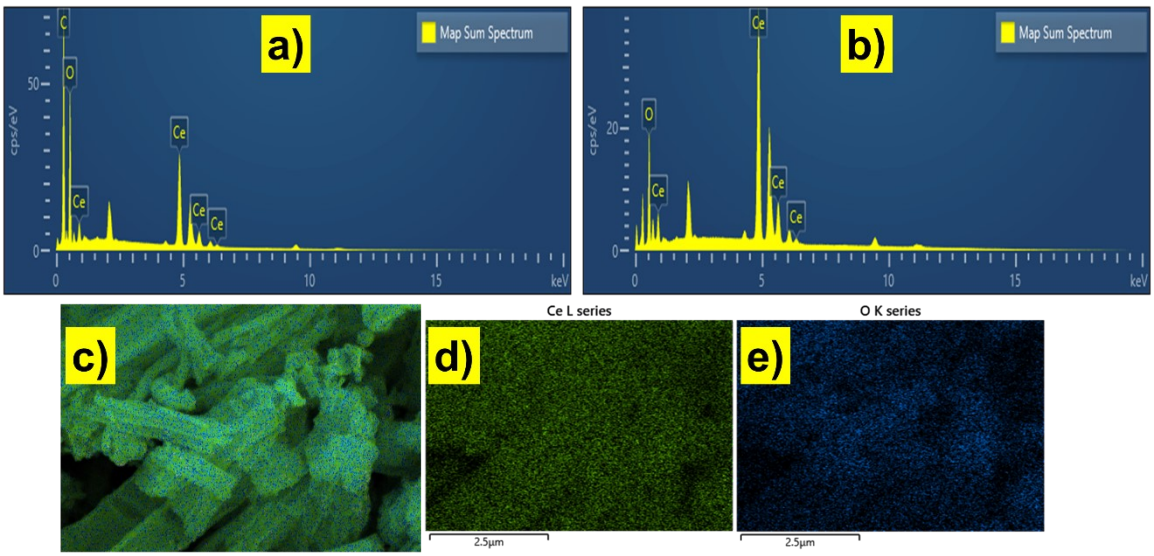


**Figure S7**. EDS for a) bare Ce-BTC MOFs, and b) bare $CeO_2$ NBs. c-e) Elemental mapping images of bare $CeO_2$ NBs.

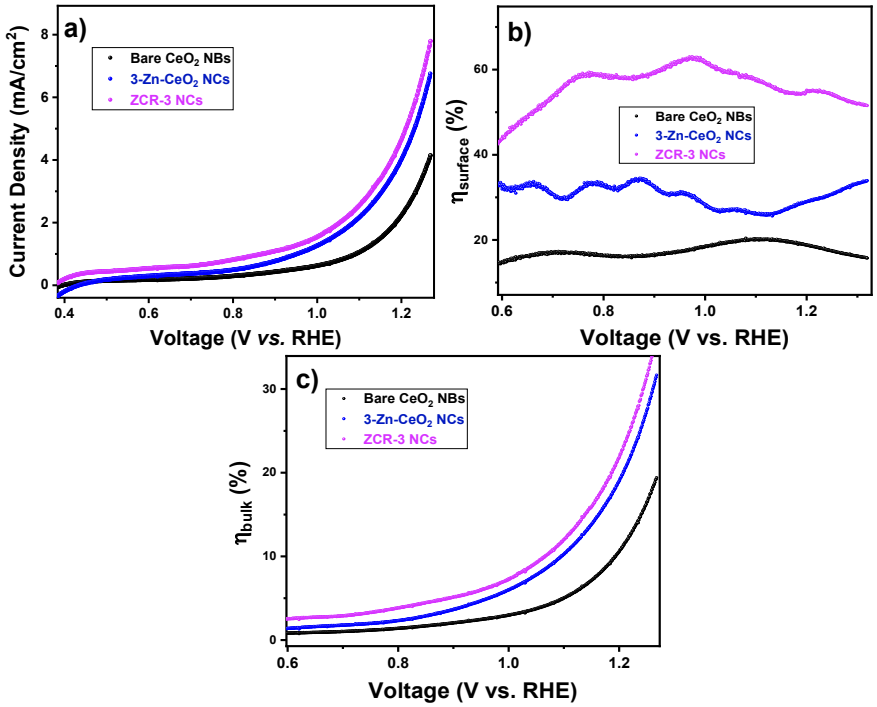


**Figure S8**. a) LSV curves in presence of scavenger ($Na_2SO_3$), b) surface charge injection efficiency, and c) bulk charge separation efficiency verses $V_{RHE}$ for bare $CeO_2$ NBs, 3-Zn-$CeO_2$ NCs and ternary ZCR-3 NCs-based photoanodes.

**Table S1**. Previously reported $CeO_2$-based photoelectrodes for PEC water splitting

| Sr. No. | Samples | Outcomes | Electrolyte | Ref. |
|---|---|---|---|---|
| 1. | $CeO_2$@Ag@CdS Nanotube arrays | 2.14 mA/cm$^2$ at −0.2 V *vs.* Ag/AgCl | 0.5 M $Na_2SO_4$ | 4 |
| 2. | ZnO@PDA/$CeO_2$ heterostructures | 251 µA/cm$^2$ at 0.25 V *vs.* RHE | 0.1 M $Na_2SO_4$ | 5 |
| 3. | $CeO_2$/$TiO_2$ Nanotube arrays | 2.11 mA/cm$^2$ at 1.23 V *vs.* RHE | 0.1 M $Na_2SO_4$ | 6 |
| 4. | Au@$CeO_2$ | 0.045 mA/cm$^2$ at 0.6 V *vs.* Ag/AgCl | 0.2 M $Na_2SO_4$ | 7 |
| 5. | ZnO-$CeO_2$-rGO NCs | 0.69 mA/cm$^2$ at 1.5 V vs. RHE | 0.1 M $Na_2SO_4$ | 8 |
| 6. | ZnO-$CeO_2$ NCs | 1.41 mA/cm$^2$ at 0.9 V *vs.* Ag/AgCl | 1 M aq. NaOH | 9 |
| 7. | **Zn-doped $CeO_2$ NCs** | **1.057 mA/cm$^2$ at 1.23 V *vs.* RHE** | **0.5 M $Na_2SO_4$** | **This Work** |
| 8. | **Zn-$CeO_2$/rGO NCs** | **2.228 mA/cm$^2$ at 1.23 V *vs.* RHE** | | |

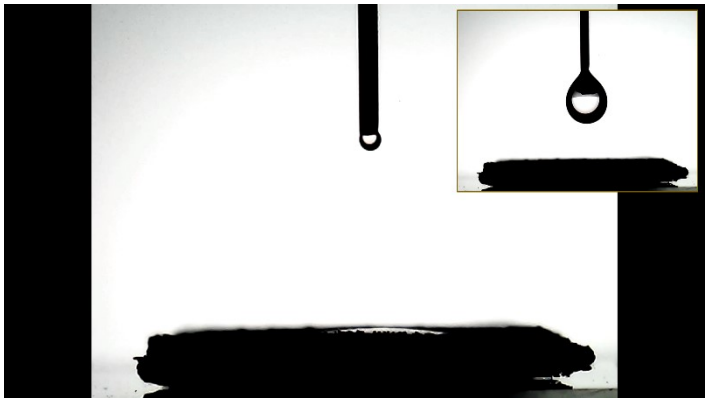

**Figure S9**. Contact angle measurement's image of ZCR-3 NCs-based photoanode (inset: image before water contact).

**References:**


1 K. Prabakaran, P. J. Jandas, S. Mohanty and S. K. Nayak, *Sol. Energy*, 2018, **170**, 442–453.

2 R. Bhargava, J. Shah, S. Khan and R. K. Kotnala, *Energy & Fuels*, 2020, **34**, 13067–13078.

3 M. E. Khan, M. M. Khan and M. H. Cho, *Sci. Rep.*, 2017, **7**, 5928.

4 M. Zhao, H. Li, X. Shen, Z. Ji and K. Xu, *Dalt. Trans.*, 2015, **44**, 19935–19941.

5 N. Celebi, F. Arlı, F. Soysal and K. Salimi, *Mater. Today Energy*, 2021, **21**, 100765.

6 S.-W. Lin, M.-H. Tong, Y.-X. Chen, R. Chen, H.-P. Zhao, X. Jiang, K. Yang and C.-Z. Lu, *ACS Appl. Energy Mater.,* **2023**, 6, 1093–1102.

7 M. M. Khan, S. A. Ansari, M. O. Ansari, B. K. Min, J. Lee and M. H. Cho, *J. Phys. Chem. C*, 2014, **118**, 9477–9484.

8 Y. Tan, S. Zhang, R. Shi, W. Wang and K. Liang, *Int. J. Hydrogen Energy*, 2016, **41**, 5437–5444.

9 A. Das, M. Patra, M. Kumar P, M. Bhagavathiachari and R. G. Nair, *J. Alloys Compd.*, 2021, **858**, 157730.